NTS-1321

SAND81-1058
Unlimited Release
Printed April 1982

Distribution
Category UC-70

In-Situ Tuff Water Migration/Heater Experiment: Instrumentation Design and Fielding

David R. Waymire
Experiments Planning Division 1112

Carl O. Duimstra
Field Instrumentation Division I, 1124
Sandia National Laboratories
Albuquerque, NM 87185

Abstract

In conjunction with the Nevada Nuclear Waste Storage Investigation Project, Sandia National Laboratories conducted a Water Migration/Heater Experiment in welded tuff at the Nevada Test Site. The heater and associated instrumentation were operated underground for about 7 months during FY80. The instrumentation measured water depth and alkalinity, temperatures, cavity pressures, relative humidity, in-situ stress changes, and displacement in the drill holes and surrounding rock mass. An on-line, calculator-based data acquisition system controlled the experiment and accumulated 120 channels of data. Most instrumentation operated satisfactorily and almost all was recovered for postmortem examination.

PORTIONS OF THIS DOCUMENT ARE ILLEGIBLE

Contents

Figures

Tables

In Situ Tuff Water Migration/Heater Experiment: Instrumentation Design and Fielding

Introduction

The in-situ Tuff Water Migration and Heater Experiment was conducted in the welded tuff of the Grouse Canyon Member, in the G-tunnel complex at the Nevada Test Site (NTS) in southern Nevada during FY80.[1] Before this test, two other field experiments had been conducted by the NNWSI Geotechnical Projects Division at Sandia National Laboratories (SNL) at Albuquerque, New Mexico. Both were full-scale near-surface heater experiments to assess the thermal, thermomechanical, and chemical responses of shales when exposed to heat. The tests would partly determine the suitability of shales as candidate host rocks for nuclear waste.

The first experiment included two heater sites located approximately 30.5 m (100 ft) apart, at different depths, and in different rock strata. The heaters, whose heated sections were each about 0.30 m (12 in.) in diameter and 3 m (10 ft) long, were positioned in the Conasauga formation on the Oak Ridge National Laboratory reservation in Tennessee.[2]

The second field experiment was with a single heater placed in the Eleana shale formation within the NTS. Data obtained from this test have been analyzed and reported.[3]

The latest experiment, the subject of this report, was designed to provide data on the generation of water and its movement in the vicinity of a heat source implanted in welded volcanic tuff.[1] The experiment focused in an alcove mined 427 m (1400 ft) beneath the top ridge of Rainier Mesa in Area 12. The array of drill holes (Figures 1, A1) was inclined upward at 20° from the horizontal. Such an incline permitted the holes to penetrate the overhead welded tuff and water to collect in the holes against the packers.

We developed the general criteria for the experiment at the end of 1978. We defined and bought a new data acquisition system (DAS) which was based on the Hewlett-Packard 9845 calculator/controller; specified power requirements; and picked transducers to monitor temperatures, pressures, stresses, pH, relative humidity (RH), and heater power.

We also designed a program to develop a stabilized, laser strainmeter and an electronic water-level sensor. The Instrumentation Development Division at SNL supplied the thermocouples, pressure transducers, and stress meters; we purchased other special instrumentation, such as pH and RH sensors and meters.

The heater was centered at a depth of 18.75 m (61.5 ft). Most of the remaining instrumentation was located within 3.0 m of the heater's center. Table 1 is a list of instrumentation and channel identifications. Results and analyses of measurements have been reported separately.[4]

In the field, we installed signal conditioning, power distribution, and the DAS in an air-conditioned, environmentally controlled alcove. Figure A2 is a photograph of the alcove, including the DAS, a telephone alarm system, and hardware for the signal conditioning system and its display. The collars for the drill hole array (Figure 1) were located at the rear of this alcove.

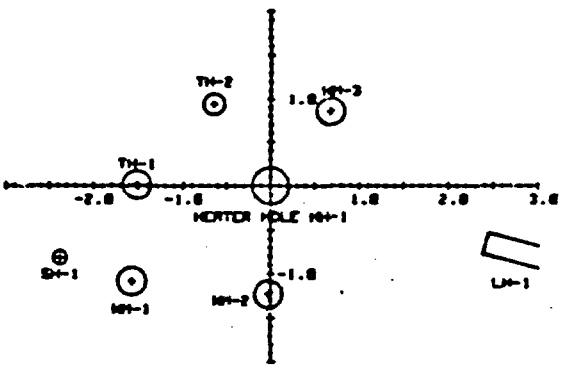

Figure 1. Experiment Hole Array Layout (at hole collar; dimensions in feet)

Table 1. Tuff Channel Identification Listing

Ch No.	ID	Gage Type	Location	Units	Calibration
0	RF-1	Reference Junc	Card 1	Ohms	SNLA
1	T-1	Type E TC 10 TCM	Heater Element E-1	°C	NBS
2	T-2	Type E TC 11	Heater Element E-2	°C	NBS
3	T-3	Type E TC 12	Insul Section Hi	°C	NBS
4	T-4	Type E TC 13	Insul Section Lo	°C	NBS
5	T-5	Type E TC 14	Junction Section	°C	NBS
6	T-6	Type E TC 15	Heater Instr Air	°C	NBS
7	T-7	Type E TC 16	Heater Instr H20	°C	NBS
8	T-8	Type E TC 6	Near Heater End 2	°C	NBS
9	T-9	Type E TC 3 TCM	Near Heater End 6	°C	NBS
10	T-10	Type E TC 9	Near Heater End 10	°C	NBS
11	T-11	Type E TC 5	Heater Midplane 2	°C	NBS
12	T-12	Type E TC 2 TCM	Heater Midplane 6	°C	NBS
13	T-13	Type E TC 8	Heater Midplane 10	°C	NBS
14	T-14	Type E TC 4	Far Heater End 2	°C	NBS
15	T-15	Type E TC 1 TCM	Far Heater End 6	°C	NBS
16	T-16	Type E TC 7	Far Heater End 10	°C	NBS
17	T-17	Type E TC 22	Near Heater Rock 12	°C	NBS
18	T-18	Type E TC	Bkgd Standard-Ice	°C	NBS
19	Cal V	Analogic	Card 1 Calibration	Volts	SNLA
20	RF-2	Reference Junc	Card 2	Ohms	SNLA
21	T-19	Type E TC 19	Near Heater Rock 4	°C	NBS
22	T-20	Type E TC 25	Near Heater Rock 8	°C	NBS
23	T-21	Type E TC 21	Mid-Heater Rock 12	°C	NBS
24	T-22	Type E TC 18 TCM	Mid-Heater Rock 4	°C	NBS
25	T-23	Type E TC 24	Mid-Heater Rock 8	°C	NBS
26	T-24	Type E TC 20	Far Heater Rock 12	°C	NBS
27	T-25	Type E TC 17	Far Heater Rock 4	°C	NBS
28	T-26	Type E TC 23	Far Heater Rock 8	°C	NBS
29	T-27	Type E TC 1	WM-1 Water 62.0 ft	°C	NBS
30	T-28	Type E TC 2	WM-1 Air 62.17 ft	°C	NBS
31	T-29	Type E TC 3	WM-1 Left 62.3 ft	°C	NBS
32	T-30	Type E TC 4	WM-1 Right 62.3 ft	°C	NBS
33	T-31	Type E TC 1	WM-2 Water 61.5 ft	°C	NBS
34	T-32	Type E TC 2	WM-2 Air 61.67 ft	°C	NBS
35	T-33	Type E TC 3	WM-2 Left 61.8 ft	°C	NBS
36	T-34	Type E TC 4	WM-2 Right 61.8 ft	°C	NBS
37	T-35	Type E TC 1	WM-3 Water 61.08 ft	°C	NBS
38	T-36	Type E TC	Bkgd Standard-Ice	°C	NBS
39	Cal V	Analogic	Card 2 Calibration	Volts	SNLA
40	Ref-2	Reference Junc	Card 3	Ohms	SNLA
41	T-37	Type E TC 2	WM-3 Air 61.25 ft	°C	NBS
42	T-38	Type E TC 3	WM-3 Left 61.38 ft	°C	NBS
43	T-39	Type E TC 4	WM-3 Right 61.38 ft	°C	NBS
44	T-40	Type E TC	TH-1 53.5 ft	°C	NBS
45	T-41	Type E TC	TH-1 56.5 ft	°C	NBS
46	T-42	Type E TC	TH-1 59.5 ft	°C	NBS
47	T-43	Type E TC	TH-1 60.5 ft	°C	NBS
48	T-44	Type E TC	TH-1 61.5 ft	°C	NBS
49	T-45	Type E TC	TH-1 62.5 ft	°C	NBS
50	T-46	Type E TC	TH-1 63.5 ft	°C	NBS
51	T-47	Type E TC	TH-1 64.5 ft	°C	NBS
52	T-48	Type E TC	TH-1 69.5 ft	°C	NBS
53	T-49	Type E TC	TH-2 56.5 ft	°C	NBS
54	T-50	Type E TC	TH-2 58.5 ft	°C	NBS
55	T-51	Type E TC	TH-2 60 ft	°C	NBS
56	T-52	Type E TC	TH-2 60.5 ft	°C	NBS
57	T-53	Type E TC	TH-2 61 ft	°C	NBS
58	T-54	Type E TC	Bkgr Standard-Ice	°C	NBS
59	Cal V	Analogic	Card 3 Calibration	Volts	SNLA
60	RF-4	Reference Junc	Card 4	Ohms	SNLA

Table 1. (cont)

Ch No.	ID	Gage Type	Location	Units	Calibration
61	T-55	Type E TC	TH 2 61.5 ft	°C	NBS
62	T-56	Type E TC	TH 2 62 ft	°C	NBS
63	T-57	Type E TC	TH 2 62.5 ft	°C	NBS
64	T-58	Type E TC	TH 2 63 ft	°C	NBS
65	T-59	Type E TC	TH 2 63.5 ft	°C	NBS
66	T-60	Type E TC	TH 2 64.5 ft	°C	NBS
67	T-61	Type E TC	TH 2 65.5 ft	°C	NBS
68	T-62	Type E TC	TH 2 67.5 ft	°C	NBS
69	T-63	Type E TC	Stress 62.3 ft	°C	NBS
70	T-64	Type E TC	Stress 62.3 ft	°C	NBS
71	T-65	Type E TC	LH-1 29.8 ft	°C	NBS
72	T-66	Type E TC	LH 2 28.7 ft	°C	NBS
73	T-67	Type E TC	Instr Alcove	°C	NBS
74	T-68	Type E TC	Laser 28.7 ft	°C	NBS
75	T-69	Type E TC	Alcove Rock Wall	°C	NBS
76	T-70	Type E TC	Instr Rack	°C	NBS
77	T-71	Type E TC	Laser Alcove	°C	NBS
78	T-72	Type E TC	Bkgd Standard-Ice	°C	SNLA
79	Cal V	Analogic	Card 4 Calibration	Volts	SNLA
80	PR 1	Pressure SN 1012	Heater Hole	psi	0.0427 V psi
81	PR 2	Pressure SN 1025	Heater Hole	psi	0.0680 V psi
82	PR 3	Pressure SN 1005	Hole WM 1	psi	0.0430 V psi
83	PR 4	Pressure SN 1017	Hole WM 1	psi	0.0482 V psi
84	PR 5	Pressure SN 1004	Hole WM 2	psi	0.0453 V psi
85	PR 6	Pressure SN 1016	Hole WM 2	psi	0.0561 V psi
86	PR 7	Pressure SN 1006	Hole WM 3	psi	0.0430 V psi
87	PR 8	Pressure SN 1021	Hole WM 3	psi	0.0458 V psi
88	PR 9	Pressure SN 1020	Alcove	psi	0.0476 V psi
89	S 1	Stress SE 28	SH 1 0° 62.75 ft	mV	SNLA
90	S 2	Stress SE	SH 1 0° 62.29 ft	mV	SNLA
91	S 3	Stress SE 27	SH 1 90° 61.5 ft	mV	SNLA
92	LAS 2	Laser Strain	LH 1	Micron	20 V 4096 ct
93	PH 1	PH Sensor RE731	Heater Hole	PH	SNLA
94	PH 2	PH Sensor RE736	Alcove	PH	SNLA
95	PH 3	PH Sensor RE540	WM 2	PH	SNLA
96	PH 4	PH Sensor RE732	WM 3A	PH	SNLA
97	RH 2	Rel Humid SN 701	WM 1	RH	TH Sn1
98	RH 1	Rel Humid SN 702	Heater Hole	RH	TH Sn1
99	Cal V	Analogic	Card 5 Calibration	Volts	SNLA
100	RH 4	Rel Humid SN 703	WM 3A	RH	TH Sn1
101	RH 3	Rel Humid SN 704	WM 2	RH	TH Sn1
102	V 1	Element Voltage	Heater Hole	Volts	SNLA
103	A 1	Element Current	Heater Hole	Amps	SNLA
104	P 1	Heater Power	Heater Hole	Watts	SNLA
105	V 2	Element Voltage	Heater Hole	Volts	SNLA
106	A 2	Element Current	Heater Hole	Amps	SNLA
107	P 2	Heater Power	Heater Hole	Watts	SNLA
108	WAT 1	Water Level	Heater Hole	Volts	SNLA
109	WAT 2	Water Level	WM 1	Volts	SNLA
110	WAT 3	Water Level	WM 2	Volts	SNLA
111	WAT 4	Water Level	WM 3	Volts	SNLA
112	LAS 1	Laser Strain	LH 1	Micron	20 V 4096 ct
113	Cal V	Analogic	Card 6 Calibration	Micron	SNLA
114	TH 1	Thermistor	TC 2 58.5 ft	°C	SNLA
115	TH 2	Thermistor	TC 2 62.5 ft	°C	SNLA
116	TH 3	Thermistor	TC 2 59.5 ft	°C	SNLA
117	TH 4	Thermistor	TC 2 69.5 ft	°C	SNLA
118	P 1D	Heater Power	Heater Hole	Watts (BCD)	SNLA
119	P 2D	Heater Power	Heater Hole	Watts (BCD)	SNLA
120	P 3D	Heater Power	Total Power	Watts (BCD)	SNLA

Instrumentation

Heater Design

The heater that we designed and fabricated for this experiment was an adaptation of previous designs used in shale experiments. The significant differences were reduced size and the elimination of air cooling for the terminal section. The heater elements themselves were 1.22 m long; this can be compared to a 3.05-m heated section in the full-scale experiments.

The heater was essentially a right cylinder that used two hairpin, electrical-resistive heating elements supplied by Chromolux and which had been used successfully in previous tests. Also, we used mechanically operated RTV silicone packers rather than air-inflated ones to seal off the holes and provide long-term water collection. The packers were expanded and squeezed to the wall by electric motors driving a metal cone through the center of an RTV ring.

Figure 2 is a sketch of the heater, instrumentation, and packer assembly. The mechanical design of the heater and other associated hardware have been reported separately.[3]

Pressure Transducers

We used pressure transducers from Gulton Industries to monitor gas pressures in Holes HH-1, WM-1, WM-2, and WM-3. Another gage was mounted in the instrumentation alcove to monitor changes in atmospheric pressure. The transducers — GS 610 Series — feature high-level (up to 5 V dc), linear variable displacement transformer (LVDT) output with infinite resolution and complete electrical isolation.

The electronics are self-contained in the same cast aluminum housing as the all-welded pressure-sensor bellows. These particular transducers are very rugged and can withstand a 50-g shock. Their response to a stepped pressure change is less than 15 ms, the proof pressure is 1.25 times the range for each type, and the burst pressure is 3.10 MPa (450 psig). Each one requires 9 to 12 V dc regulated input voltage and a maximum input current of 30 mA.

We mounted two pressure transducers in each of the heater-array holes. One was a Model GS-613-15-3-S, with a pressure range of from 0 to 0.10 MPa (0 to 15 psig) and a temperature operating range of from -18° to +82°C. The other transducers in each hole and the one in the alcove were Model GS-613-09-25, rated for 0 to 0.69 MPa (0 to 100 psig). Table 2 presents the calibration data for the four 0.10-MPa transducers and Table 3 for the five 0.69-Pa gages.

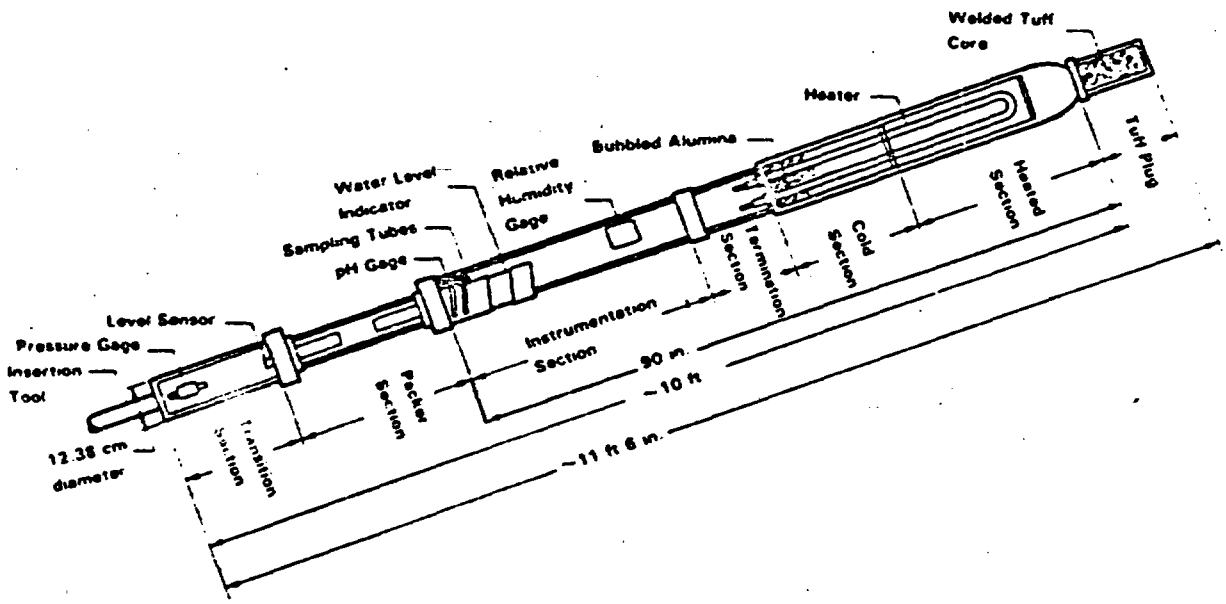

Figure 2. Heater Assembly Including Heated, Insulated, Junction, Instrumentation, Packer, and Pressure Transducer Sections

Table 2. Calibration Data for GS-613-15-3-S Pressure Transducers (Transducer output in volts)

Psig	HH-1 (S/N 1002)	WM-1 (S/N 1005)	WM-2 (S/N 1004)	WM-3 (S/N 1006)
0.0	0.811	0.768	0.756	0.740
1.5	0.875	0.834	0.822	0.805
3.0	0.939	0.897	0.886	0.868
4.5	1.002	0.960	0.950	0.931
6.0	1.064	1.024	1.012	0.994
7.5	1.128	1.087	1.077	1.056
9.0	1.192	1.151	1.141	1.122
10.5	1.255	1.215	1.205	1.185
12.0	1.318	1.278	1.267	1.249
13.5	1.445	1.406	1.398	1.377

Table 3. Calibration Data for GS-613-09-25 Pressure Transducers (Transducer output in volts)

Psig	HH-1 (S/N 1025)	WM-1 (S/N 1017)	WM-2 (S/N 1018)	WM-3 (S/N 1023)	Alcove (S/N 1020)
0	0.165	0.049	0.097	0.054	0.123
10	0.645	0.532	0.577	0.546	0.598
20	1.125	1.011	1.059	1.018	1.077
30	1.615	1.492	1.552	1.512	1.562
40	2.102	1.982	2.043	1.995	2.046
50	2.592	2.471	2.535	2.486	2.536
60	3.082	2.961	3.028	2.977	3.039
70	3.571	3.449	3.522	3.469	3.532
80	4.057	3.936	4.014	3.960	4.023
90	4.542	4.420	4.505	4.446	4.515
100	5.025	4.902	4.994	4.933	5.007

Before we installed the transducers in the field, they were calibrated at the SNL Standards Laboratory. The sensitivity and offset of each individual transducer were used in the automatic DAS to convert transducer output into pressures in lb/in^2. In the field, we mounted them inside an open steel canister on the alcove-side of the packer section of the drill holes. A stainless steel tube connected the pressure port to the sealed cavity beyond the packers.

After several months in this environment, transducers S/N 1005 in Hole WM-1, S/N 1004 in Hole WM-2, and S/N 1018 in Hole WM-2, started behaving erratically. During the cooldown phase of the experiment, S/N 1004 stabilized at about –0.05 MPa (–7.0 psig), S/N 1005 at –0.04 MPa (–5.5 psig), and S/N 1018 at –0.02 MPa (–2.7 psig).

During the postmortem, the pressure cavity and bellows of all transducers appeared to be functional and in good condition. However, the output sensitivity of the three erratic gages had decreased and they drew about twice the input current as the other units. The electronics on all units showed effects of humidity and corrosion, especially those that had behaved erratically, whose effects were severe enough to short out resistors, damage transistors, and cause other damages. In the future, it would be advisable to encapsulate the electronic section with some type of humidity- and temperature-resistant material.

Alkalinity Sensor

The pH of the water collected in the holes was to be measured in situ, using small gel-filled sensors. They were mounted on brackets in the instrumentation compartment, just beyond the deep packer. Here, the electrode tip would be immersed in water as it pooled behind the packer.

We used the Sensorex® Model S10CC sealed reference combination pH electrodes with a 23-m (75-ft) cable lead and standard Beckman connectors. Their small size allowed them to be mounted in the space available for instrumentation. Their rugged polymer body protected the fragile tip from damage during mounting and insertion.

The pH meters were Model NX digital readout instruments supplied by Sargent-Welch Scientific Co. This particular meter has a relative accuracy of ±0.01 pH over the pH range of from 0 to 14. The repeatability is also ±0.01 pH. The recorder output is 1 mV/pH with ±1% accuracy. Separate slope and intercept controls are also provided and temperature compensation is either manual or automatic, as desired. Both calibration and standby modes are also available. The calibration mode is used in conjunction with slope, intercept, and temperature controls to calibrate the meter, using buffered solutions. Standby is used to disconnect the reference jack from the circuit and to connect the intercept voltage only across the digital voltmeter (DVM) terminals. This mode is used when electrodes are not immersed.

When we were assembling the sensors at NTS, an electrical short occurred in the potted section of the pH cable in the WM-1 package and the pH level was not measured in this hole. Instead, the meter designated for WM-1 was connected to another Sensorex electrode in the alcove. Whenever we took water from a drill hole, we measured the pH in the alcove to cross-check the in-situ measurements. We considered this cross-checking advisable because in-situ probes could not be cleaned, stirred, or recalibrated once they had been inserted; they remained in place for 7 months.

At the beginning, each meter was adjusted and calibrated with the electrodes that were to be actually inserted into the holes. Standard buffered solutions of 4, 7, and 10 pH were used for calibration. The electrodes were then disconnected and a standard cell connected to the meters. This cell had been calibrated at SNL Standards Laboratory for output accuracy. The meter output for standard cell settings of 4, 7, and 10 were recorded for future meter adjustments.

The leads from the in-situ electrodes were periodically removed from the meter's input terminals during the in-situ test and the meter connected to the standard cell. We could then adjust the slope and intercept controls to restore the pH meter to the calibrated values in case it had drifted. However, we noted no significant drift throughout the experiment.

Calibration data for the sensors and meters are listed in Table 4; PH-1 refers to the measurements from HH-1, PH-2 to the electrode and meter used for measuring in the alcove, and PH-3 and PH-4 to the WM-2 and WM-3 respectively. The "R" numbers in each column refer to the SNL property numbers of each meter.

Table 4. PH Meter Calibration Data

pH	PH-1 (R11713)	PH-2 (R11714)	PH-3 (R11840)	PH-4 (R11712)
Buffered Solution				
4	4.00 ± 0.02	4.00 ± 0.02	4.00 ± 0.02	4.00 ± 0.02
7	7.00 ± 0.02	7.00 ± 0.02	7.00 ± 0.02	7.00 ± 0.02
10	10.00 ± 0.02	10.00 ± 0.02	10.00 ± 0.02	10.00 ± 0.02
Test Cell Setting				
4	4.05	4.30	4.28	4.28
5	5.16	5.36	5.30	5.30
6	6.24	6.43	6.32	6.32
7	7.32	7.50	7.34	7.34
8	8.39	8.57	8.37	8.36
9	9.47	9.63	9.39	9.39
10	10.56	10.70	10.41	10.41

Laser Strainmeter

A Tropel® Model 100, single-frequency helium-neon laser was used as a strainmeter to monitor small displacements caused by thermomechanical effects in the rock mass surrounding the heater. (Other experimenters have also used such interferometers as strainmeters.[4]) The meter consisted of the laser source, mirrors, vacuum pipe with quartz windows, "cat's eye" lens, and photodiode detectors (Figure 3). We mounted the laser on a flange fastened to the borehole collar and viewed the cat's eye through the line-of-sight vacuum pipe. Fringes, that is, displacements detected by the photodiodes, were counted by an electronic counting circuit.

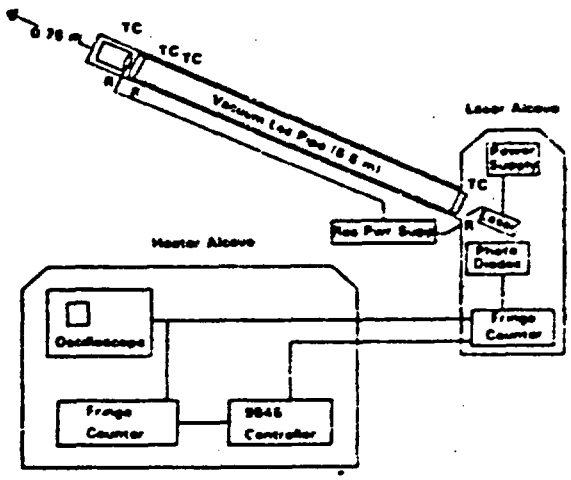

Figure 3. System Diagram for the Laser Strainmeter (Thermocouple locations are indicated by TC, and resistor locations by R.)

The laser operated at a wavelength of 632.8 nm with a nominal output power of 0.7 mW. Monitoring the laser's output frequency permitted dc-coupled control of the laser cavity length and active stabilization of the laser frequency. The laser tube used was Coherent® Model 80, with a polarized output beam.

The fringe sensing device was a silicon photo field effect transistor (photoFET) that combines a sensitive silicon photodiode and a low-noise FET. When light strikes it, photo current flows in the gate circuit, causing a positive voltage rise at the gate. PhotoFET output from two channels is then combined in an X-Y fashion. Whenever the combined signal crosses either the X or Y axis (X or $Y = 0$), a count is registered in an electrical octal-coded counter. The sense of rotation is also maintained such that counts are automatically added or subtracted as appropriate. The output of the digital counter could be recorded by the HP9845-based DAS through the RS-232C interface or through a digital-to-analog (D-to-A) converter. These interfaces could also be used to send calibration data to the DAS. Calibration function switches were also available on the electronic fringe counter, which was designed jointly by SNL and EG&G-Kirtland. Digital counts, and therefore analog voltages through the D-to-A converter, could be stepped or ramped to desired levels. Figure A3 shows the laser head and counting electronics fielded in the laser alcove.

We attempted to protect the electronics from effects of humidity by blowing tunnel air into an alcove at the end of the laser drift, a Brattice cloth sheet providing the only barrier to the alcove. In addition, two dehumidifiers were placed next to the fringe counter.

We strapped an energized resistor to the pipe flange that held the quartz window at the location of the cat's eye and its heat prevented the window from fogging. For diagnosis thermocouples (TCs) were placed at the window, next to the cat's eye, and at the laser optical head.

Inspite of our enclosing the laser head for protection, several problems occurred. Electronic components failed in the fringe counter, which was installed in the laser drift. Shorts and counting errors also occurred which were presumed to have been caused by humidity. The interferometer system also appeared to be sensitive to changes in temperature, humidity, and air currents. We do not yet know if this is true only to the extent that these changes affected some critical length in the measurement system.

Because of difficulties, we placed a fringe counter of improved design in the air-conditioned instrumentation alcove and connected it in parallel with the original counter. When we compared data from both counters, we found few discrepancies. Both recorded the same rapid, extreme, short-term excursions seen whenever recordable environmental variations occurred in the laser alcove. Recording the same phenomena indicates that they were the output of the laser itself and not caused by the counting electronics. The two counters tracked each other quite consistently, indicating that the counters were operating correctly. Slight deviations from each other, however, suggest that each was sensitive in its own way to random noise.

EG&G-Kirtland conducted laboratory tests to determine if environmental effects could influence the stability of the laser and of fringe-counting detectors. They varied temperature and barometric pressure,

but noted no significant effect. They compared three laser systems in a Fabry-Perot interferometer to check for sensitivity variations, but none was detected.

The reason for these results is probably that the laser and photodiode detectors operated as expected although there were long-term drift effects associated with the counters' sensitivity to random noise pulses. These effects can be substantially reduced to acceptable limits with improved electronics design and packaging, but probably can never be totally eliminated.

The cause of the rapid excursions in the output counts was probably the intermittant drying and resaturating of the rock wall on which the laser head was mounted. These phenomena could have been caused by any environmental changes which would have changed the humidity in the laser alcove, such as ventilation. Further laboratory tests are being conducted with a laser interferometer and welded tuff core samples to determine if this conclusion is correct.

The laser strainmeter shows great potential for measuring small displacements such as we expected in this experiment. Improvements should be made to seal the counting electronics to the environment and to eliminate operator adjustments in the fringe counting system. Improved electronics could also increase the resolution beyond the λ/8 limit. However, in spite of any new advances that may be made, a major question remains: How should the interferometer be mounted to the rock? One possibility would be to mount the laser head reference several feet into the drill hole and thus avoid surface effects due to stress relief and rock saturation. This problem may remain a major source of uncertainty in laser strainmeter measurements in the future.

Stressmeters

Commercially supplied borehole-inclusion stressmeters were modified substantially at SNL with an extended platen design,[7] and they were modified for straingages in order to make them compatible with conventional data logging equipment. These changes proved advantageous in the experiment. Other designs that use vibrating wires require special digital readout electronics, which would cause increased usage of special digital (BCD) interfaces. Figure 4 is a schematic of the mechanical design.

We placed three stressmeters in Hole SH-1 at different depths (Table 1). The two deepest meters were mounted to read horizontal stresses (radially to the heater hole), and the shallowest was oriented vertically, tangential to the heater hole. Originally, the center meter was to be oriented at 45° from the horizontal, but an equipment malfunction caused us to believe that the deepest stressmeter had not seated properly, so we oriented the second meter horizontally to yield that important data. Later, we corrected the equipment malfunction, but the stressmeter remained in the horizontal direction.

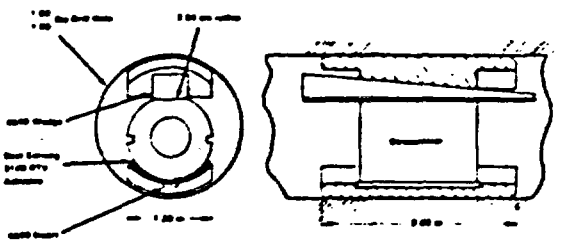

Figure 4. Mechanical Design of Stressmeter

We installed the stressmeters as soon as the stress hole was drilled, in order to watch any long-term relaxations and see if subsequent drilling in the hole array and mining of the laser drift affected the stress significantly. We also placed a TC in the stress hole to collect temperature correction data if it should prove useful.

We installed the stressmeters with an insertion tool that uses hydraulic pressure to drive a wedge, thus preloading the platen against the rock to provide a solid anchor. Preloading is also necessary in case thermal expansion due to heat should cause the hole to open. We did not remove the stressmeters after the experiment because the wedge is designed to break at a predetermined load.

The stressmeters were calibrated in a universal testing machine to indicate their output when a load (force) is applied to them. (Figure 5). These calibrated solid block data were then used to obtain stress vs force data from welded tuff block tests (Figure 6). Bridge excitation on all channels was maintained at 18.0 V dc.

The stressmeters all operated as expected. After initial voltage changes caused by stress relief from gage preloading in the borehole, we saw no other effects of stress relief before the power was turned on in the heater. Data from the stressmeters (Figure 7) shows that transducer output dropped below preload values after the heater was turned off, indicating the

importance of preloading the meters to keep them anchored. We had gained such experience in previous tests conducted in shale.

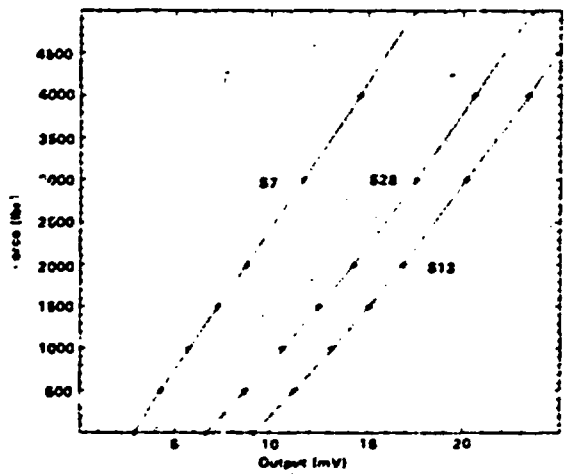

Figure 5. Force vs Output Calibration for Stressmeters S7, S13, and S28

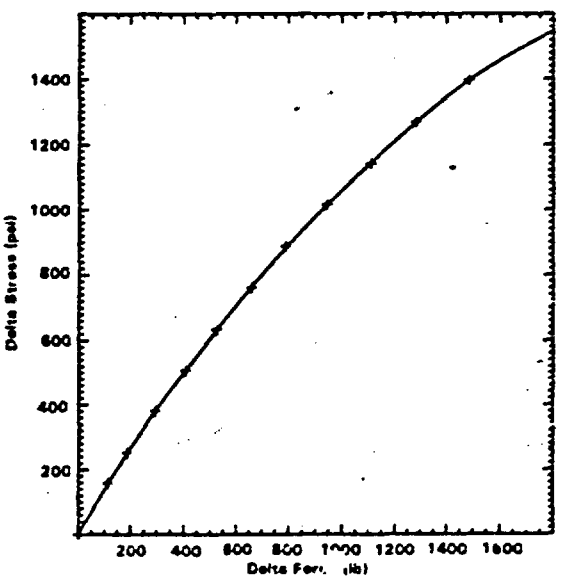

Figure 6. Delta Stress vs Delta Force for Stressmeter in a Block of Welded Tuff (tested in the laboratory)

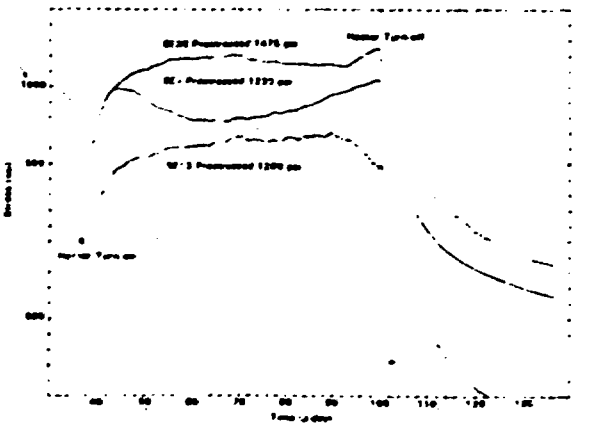

Figure 7. Actual Stressmeter Data (SE28 and SE7 were oriented radially to the heater. SE13 was oriented tangentially.)

Data Acquisition System

The DAS that we used was based on the Hewlett-Packard 9845T calculator/controller. The system was basically the HP3052A that utilizes the HP3455A programmable digital multimeter, two HP3495A scanners with low thermal and TC reference assemblies, and the HP98035A real-time clock for interrupts (Figure 8). System software for the field experiment is detailed in Reference 8.

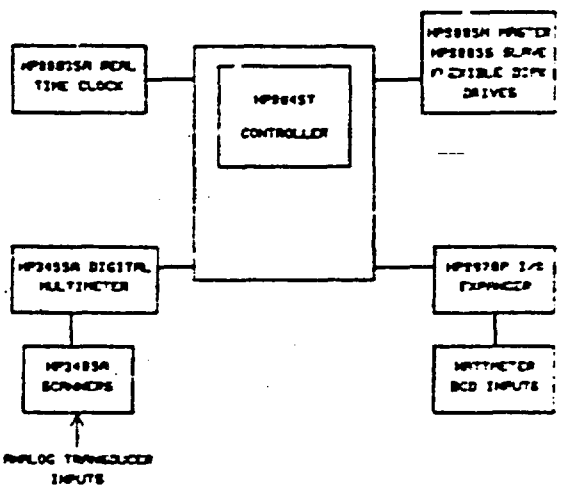

Figure 8. Block Diagram of the In-Situ Tuff Water Migration/Heater Field Experiment Data Acquisition System

Analog voltage or resistance sources were wired directly to the scanner's plug-in assemblies. On an interrupt signal from the real-time clock, the 9845T controller commanded the scanners to close selected relays sequentially, and the digital multimeter monitored the voltage level or resistance from each channel. The multimeter output was then stored in arrays in the controller's memory. These data were later stored on cassette tapes and flexible magnetic disks and, even later, retrieved for analysis.

Thermocouples were connected to relays numbered 1 through 19 in each TC reference card; Channel 0 was hardwired to a thermistor attached to an isothermal connector block. Resistance readings of the thermistor permitted the calculator/controller to determine the reference junction temperature. As the individual TC voltages were scanned and monitored, polynomial fits were performed to determine the TC junction temperatures. We discuss TC specifications in detail later in this report.

Each plug-in assembly thus included 20 channels of three-pole, low-thermal, dry-reed relays. The relays featured break-before-make operation, with contacts rated to 42-V peak voltage and a current of 40 mA (noninductive). Maximum input voltages were 42-V peak between any two terminals and 42-V peak from guard to chassis. Switching time is 1-ms maximum with greater than 10-MΩ resistance between high and low. There is also less than 1-μV differential EMF thermal offset between high and low for ambient temperature changes of ±1°C. Thermistor accuracy is specified to be ±0.2°C. A steady-state temperature gradient along the terminal from the reference temperature is less than 0.1°C maximum for ±1°C ambient temperature deviations.

Analog signals from stressmeters, thermistors, pH meters, voltage standards, laser interferometer, RH sensors, power meters, and water-level indicators all came into 20-channel low-thermal relay assemblies. Operation, voltage ratings, thermal offset, isolation, and switching time specifications for these low-thermal assemblies were all the same as for the 19-channel TC assemblies. In fact, the two assemblies are identical except for the replacement of Channel 0 by the thermistor reference in the TC assembly.

Each 3495 scanner could hold four plug-in assemblies for a total capacity of 80 channels of relays.

The HP3455a digital multimeter features up to 6 1/2 digit resolution. It is a fully guarded integrating multimeter capable of measuring dc voltage, rms ac voltage, and resistance. It is IEEE-488(1975) programmable and includes an autocalibration, removable reference assembly for dc and resistance calibration.

Up to 24 readings per second on dc measurements is possible with 1-μV sensitivity. Input resistance is greater than 10 billion ohms from 0.1- to 10-V dc ranges. Normal mode rejection at 60 Hz is greater than 60 dB. Maximum input voltage ratings are 1000-V peak between high- and low-input terminals, 500-V peak from guard to chassis, and 200-V peak from guard to low terminal. Binary coded decimal (BCD) data from the Magtrol® powermeters was also recorded, using the DAS, through the HP98033A BCD interfaces that plugged directly into the 9845.

The HP98035A real-time clock provides calendar and time-of-day information. The clock can interrupt the system at programmable intervals and at selectable times-of-day for pacing data acquisition.

The HP9845T controller used enhanced BASIC language with 448 Kbytes of read-write memory. A 30-cm (12-in.) cathode ray tube (CRT) screen displayed data and commands. The CRT can display 24 lines of 80 characters each as well as perform full graphic and plotting. An 80-character internal thermal line printer that prints 480 lines per minute is also a feature of the 9845T. The 9845T also features dual-tape cartridge drives, with 217-kbyte capacity for each tape and a tape-data transfer rate of 1440 bytes/s.

The system used the HP98432A input/output (I/O), HP98437A graphics, and the HP98431 mass storage read only memory (ROM) options. In addition to the dual tape cartridge drives, we added a dual flexible disk drive system, the HP9885M master and HP9885S slave, to enhance data storage capabilities. The drives are random access, removable, mass-storage devices with a capacity of up to 500 kbytes per disk. Double-density read write enhances the rate of access and increases storage capacity. The system also features a write-verify operation to ensure that data recorded on the disk are identical to the source information in the 9845 memory. A file-by-name system maintains user files in a directory. The disk rotates at 360 rpm, average access time is 267 ms, and transfer time is 11.1 ms per record at a rate of 23 kbytes/s.

A four-pen microprocessor-based plotter, the HP9872A, made data graphs. The HP9872A is completely programmable through the IEEE-488 bus. Its plotting area is 280 mm in the Y-, and 400 mm in the X-direction. Addressable resolution is 0.025 mm with an accuracy of ±0.2% of deflection ±0.2 mm with a repeatability of 0.04 mm. The pen speed is programmable up to a maximum of 360 mm/s, and printing speed is typically three 2.5-mm characters per second.

Relative Humidity Indicator

We did not know if water would, in fact, collect against the packers in the instrumentation holes. If it did not, or if ambient conditions prevented the liquid phase, we decided it would be valuable to use RH sensors as a backup to measure the presence of and changes in moisture content. Initial thermal-modeling calculations indicated that the instrument section in the heater hole and the water collection hole, at a radius of 0.61 m from the heater, would remain below 100°C during the experiment. Therefore, that is where we decided to install the RH sensors.

The only commercial RH sensor that could fit into the holes and withstand 80°C was Thunder Scientific Corp's hybrid HS2CHDT-2A, modified for 100°C with Option 21. We bought two complete sensor systems, including linearizing circuitry, read-out units, and spare transducer with accompanying circuitry. (Reference 9 gives specifications and operating instructions.)

During procurement, additional modeling indicated that Holes WM-2 and WM-3, at about 0.2 m from the heater would not reach 100°C. Three transducers had already been ordered and we ordered another one so that RH sensors could be installed in these two holes as well. Problems in delivery and in high-temperature calibration caused us to relax the temperature criteria for two transducers from 100° to 60°C—the standard design temperature for Thunder Scientific's sensors.

The Physical Standards Laboratory at SNL calibrated two of the original transducers. The third failed at the beginning of calibration and had to be returned for repairs. The pretest calibration data for the two transducers are shown in Tables 5 and 6, in which the measured RH is listed as a function of temperature and reference RH. The third transducer, repaired, and the fourth, ordered later, arrived during the field assembly at NTS and were checked only to see if they worked, and compared with the calibrated transducers at the ambient humidity and temperature; the two were specified to operate to 60°C.

During assembly, we checked both temperature and humidity readouts from the sensors. In order to get the transducer into the experiment package, we had to cut and splice the cables, at which time all four channels appeared to be functioning, so we did not perform another functional test in the tunnel before inserting the sensors into the drill holes; no readout electronics were available in the tunnel at that time.

Table 5. Pretest Relative Humidity Calibration Data for S/N 501

	Temperature (°C)				
Ref. RH	15.6	21.2	32.2	43.3	54.4
3.8	0.1	3.8	3.2	4.3	11.1
10.0	5.5	8.8	10.0	12.6	19.3
20.0	15.5	17.6	-	-	-
30.0	26.0	28.4	35.8	39.4	44.3
50.0	43.9	45.5	55.8	58.0	60.4
60.0	-	54.6	-	-	-
70.0	62.7	64.6	72.3	-	66.4
80.0	72.3	76.1	78.9	-	-

Table 6. Pretest Relative Humidity Calibration Data for S/N 502

	Temperature (°C)				
Ref. RH	15.6	21.1	32.2	43.3	54.4
3.8	4.8	8.7	7.4	9.0	12.1
10.0	10.7	14.0	14.5	17.1	20.4
20.0	19.6	21.4	-	-	-
30.0	28.2	29.8	36.1	40.6	44.2
50.0	45.2	45.8	55.5	60.1	61.5
60.0	-	54.5	-	-	-
70.0	64.9	64.2	72.0	-	68.5
80.0	75.0	75.4	78.8	-	-

After we had installed all the instrument packages and connected and checked out the DAS, we found that only two of the four RH channels were functioning properly; this was before any temperature change due to heater power. The two working channels read above 100% RH because the transducer had been saturated with moisture, which we were aware of. On examining them at this time, we discovered that none of the transducer linearizing circuits were wired according to the drawings supplied by the manufacturer.[9] This may have caused electrical damage to one channel when we were assembling them in the tunnel.

When we discovered this problem we deemed it unwise to completely dismantle the pipe strings and retrieve each experiment package from the drill holes

because of the risk of damage to other more important gages during retraction, disassembly, re-assembly, and re-inserting. We felt that prospects were not good for repairing transducers in a reasonable time even if the experiment were dismantled. Therefore, we made no attempt to remove them, although we did try several times to correct the problem at the linearizing circuit mounted in the alcove.

During the experiment it appeared as if one transducer operated normally. Another recovered from saturation for a few days and yielded usable data. It then became erratic and appeared to be resaturated for the remainder of the experiment.

When we recovered the instrumentation after the experiment, we sent the transducer that apparently operated properly to Physical Standards Laboratory for posttest calibration (Table 7). The other three were returned to the manufacturer who, upon analyzing stated that the transducer that operated sporatically during the test was still operational, and that the other two had suffered high-temperature damage. However, our TC data indicate that none of the transducers experienced temperatures over 77°C, which was about 23°C below the operating temperature specified in the original purchase agreement. Moreover, the transducers had failed at room temperature before the heater was turned on.

Table 7. Posttest Relative Humidity Calibration Data for S/N 502

Ref RH	Temperature (°C) 21.1	54.4
[illegible]	-28.0	-0.2
[illegible]	-18.0	11.0
[illegible]	6.0	-
[illegible]	(26.0,34.0)	49.5
[illegible]	73.0	57.3
[illegible]	83.4	-
-	-	76.8
-	101.3	-

[illegible] pretest calibration data in Table 6

Water-Level Indicator

[illegible] search failed to find a commercially [illegible] water [illegible] sensor that could measure in [illegible] and small enough to fit into a [illegible] a sensor was required to measure the presence of water and to provide water-collection-rate data from the holes. We undertook a development program to design and build a sensor meeting these criteria. Several schemes were proposed and tested:

- Fluid/air conductivity differences
- Float and tilt indicators
- Air flow through the liquid
- Change in index of refraction in air and water.

The first model tested for conductivity differences had carbon pencil lead as electrodes. We used ordinary tap water as a reasonable approximation of tuff water. We also ran tests with distilled water, salt brine, and distilled water equilibrated with pulverized tuff samples. For soldering, we coated one end of the carbon leads with a flash coat of copper and, at first, used a pin spacing of 2.54 mm (0.1 in.). However, preliminary tests indicated that surface tension and wetting caused problems when the pins were that close, so we doubled the spacing, solving this problem. In addition to the 13 pins required to provide a 63.5-mm (2.5-in.) range, we used two other pins to measure conductivity of the water, thus requiring two separate circuits (Figure 9).

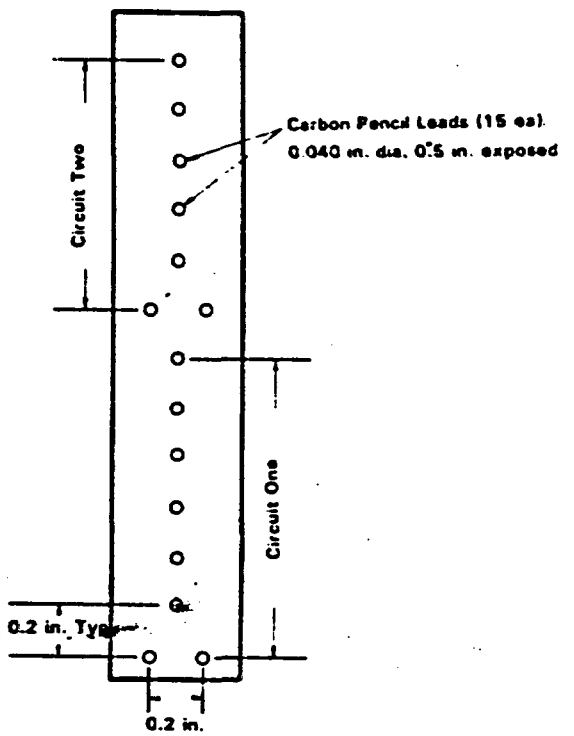

Figure 9. Pin Layout of Preliminary Water-Level Probe

Twice we attempted to mold prototype gages in this configuration, but the lead electrodes repeatedly broke. Tests in a very humid environment also indicated that, for this proposed geometry and design, condensation and moisture led to conductivity changes similar to those experienced with complete submersion.

Because of these problems, we decided to design a float-type sensor with tilt gages that had a ±12 angular degree range and the capability of measuring 63.5 mm of water in a 127-mm (5-in.) hole. Friction drag on bearings, possible corrosion and clogging of bearings, and minimum water depth required for bouyancy caused us to abandon this scheme.

Although hardware was purchased for index-of-refraction measurement of water depth, two considerations caused us to abandon this method. Each sensor could measure only the presence of water at one depth, therefore, several sensors with associated cables and electronics would be needed for each hole. Water conditions and purity in the field were not known and it was possible that a glass probe would be coated with mineral deposits, possibly leading to erroneous indications of presence of water in the holes.

An air-bubbling scheme was also not pursued as feasible. Several air tubes would have been required for each hole and pressure or flow diagnostics and electronics would have been extensive, cumbersome, and costly. We also felt that the method would not have been very accurate for the low levels of water expected. We therefore redirected design efforts to schemes of electrical conductivity measurement with hope of improving the method. Pins were made of gold wire to prevent breaking and corroding and were spaced 12.70 mm (0.5 in.) apart to mitigate surface tension and wetting problems. The way we arranged the pins (Figure 10) allowed us to measure water level at 6.35-mm (0.25-in.) intervals. Laboratory measurements, using the circuit shown in Figure 11, indicated that we could measure 10 discrete, repeatable steps with voltage steps of 300 to 400 mV per step. Figure 12 presents final calibration data for the four probes.

In spite of the encouraging calibration data for these probes, we knew potential problems existed. One major concern was the possible coating of the pins and teflon holder with material, either conducting or nonconducting, which could change the voltage output of the sensor as a function of water depth. We hoped that, in this case at least, a voltage change, even if different from the calibration steps, would indicate submersion of individual pins. Temperature, humidity, and other chemical effects on the hardware were other concerns.

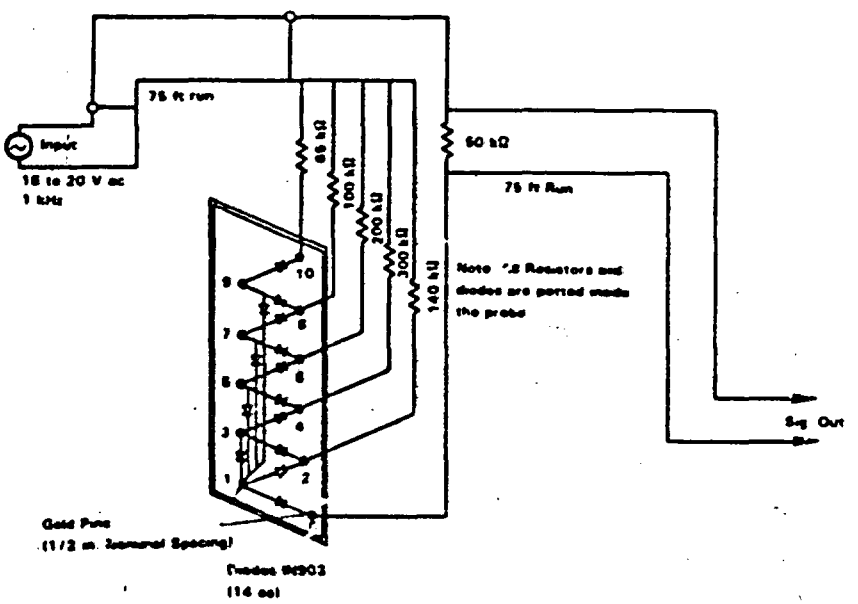

Figure 10. Pin Placement of Water-Level Probe

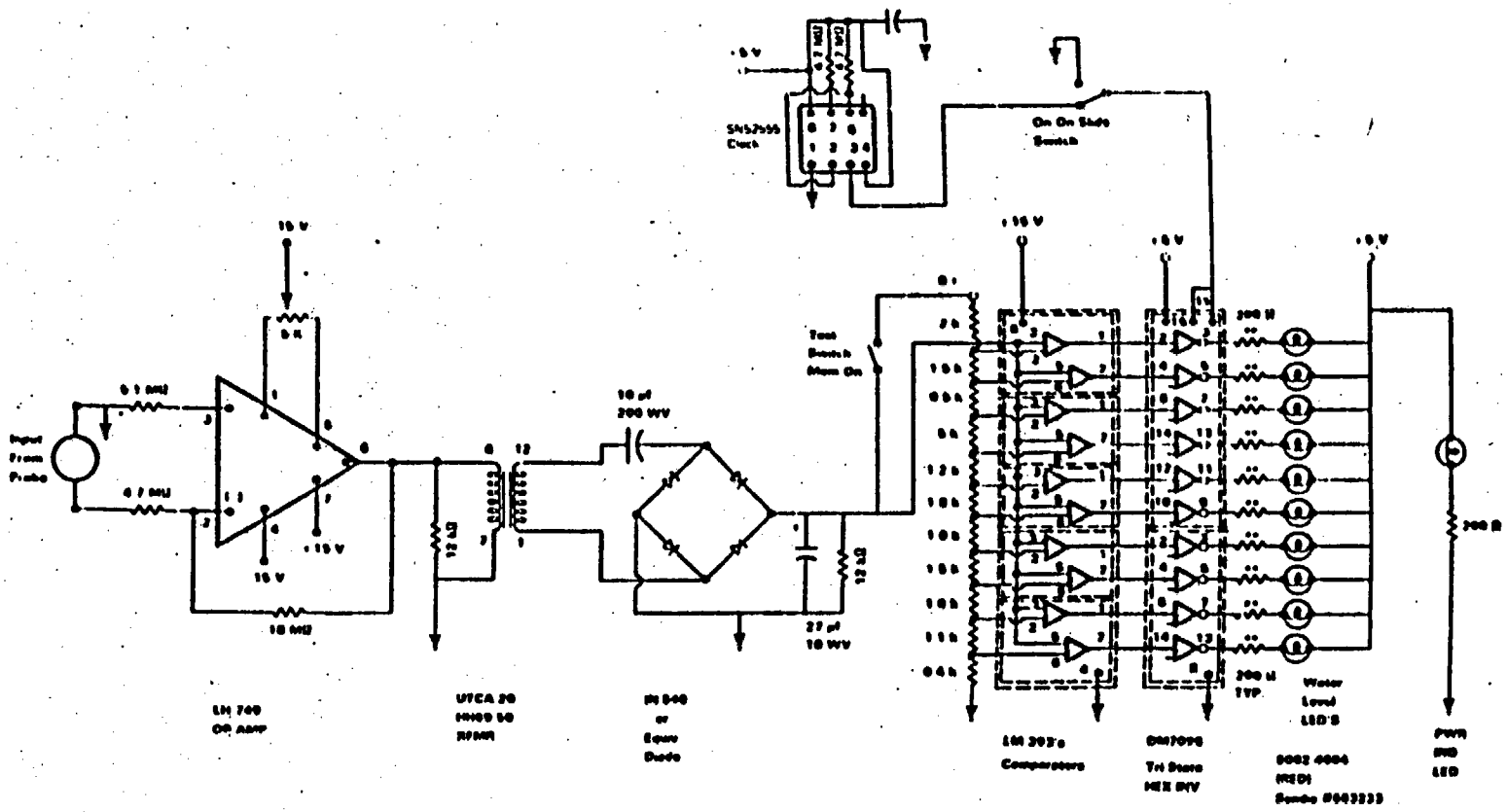

Figure 11. Water-Level Output Indicator Schematic

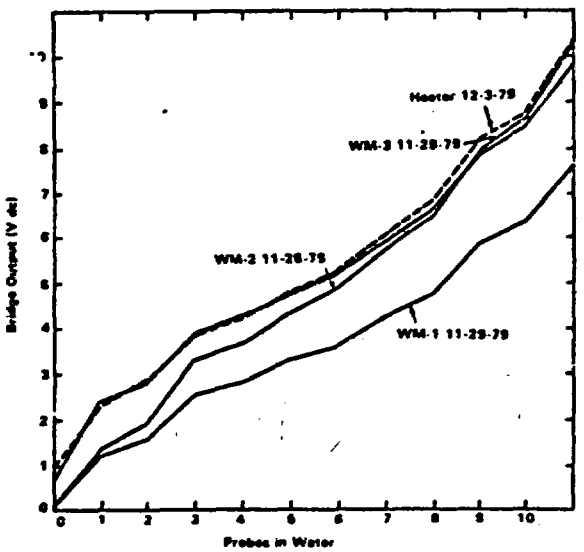

Figure 12. Calibration Data for the Water-Level Indicator

Major circuitry features of the water-level sensor are the following:

- The gage is excited by a 1-kHz sine wave, 20.5 V peak to peak for the heater hole and 18.5 V for the water-migration probes.
- As the various gold pins are submerged, the steering diodes are shunted in turn, allowing conduction from pin to pin through a series resistor. Each time an additional pin is submerged the ac signal level increases.
- The output signal from the probe is fed into a high-impedance operational amplifier (LH-740) operating as an emitter follower with unity gain.
- The signal out of the amplifier is transformer-coupled through isolation transformers (UTC A-20) to a full-wave bridge rectifier.
- The dc signal resulting from rectification is then fed into 10 comparators (LM-393).
- Each comparator has a fixed reference voltage that is applied to one side; as the voltage level increases from the bridge circuit, additional comparators are turned on.
- The output of the comparators are then routed to light-emitting diode (LED) displays, the HP9845, and individual DVMs through buffered outputs.
- A clock (S/N 52555) was added to provide the option of blinking light display to alert the operator to a water-level indication.

As originally designed and calibrated, a separate light came on as each pin was submerged. However, the light display in actuality was tied only to the comparator voltages and was only an indication of voltage. If the water conductivity was different from that of the calibration water, input excitation voltages varied, or coating of the pins occurred, the light display may not be a true reading of pin submersion. In such a case the DAS should at least indicate steps in voltage corresponding to water level.

The water-level sensors performed well during the 7-month burial. Some of the effects mentioned above were present and affected the light display. When first installed the signal output yielded discrete steps when pins were submerged. As the experiment progressed the steps became less distinct and sometimes we found it difficult to determine which pins were actually submerged.

In spite of these problems, the water-level indicators did give us enough information for collecting and draining the water collected during the field experiment.

At the time the instruments were recovered, a coating of yellow slime was found in the holes up to the level where water had been standing (Figure A4). We do not know the source or the chemical composition of this material, but possibly it was at least partially responsible for the observed behavior of the sensors.

Thermocouple Instrumentation

In addition to the rather extensive TC monitoring of temperatures in and around the main heater hole and the three water migration holes, TC strings were also installed in two temperature holes, TH-1 and TH-2 (see Figure 1). Originally both TC holes were to have been drilled to size NQ 75.7 mm (2.98 in.) but because of drilling problems, we used a 96-mm (3.78-in.) HQ hole initially intended for water migration; we designated this hole TH-1.

We made TC strings for each of the TC holes by using 3.17-mm (0.125-in.), stainless-steel 304-sheathed, chromel-constantan TCs. In addition to the TCs, two thermistors were installed in each string for comparison and as a field test of their ruggedness.

We expected difficulties and uncertainties when securing the TCs in with grout or sand in slightly upward-inclined holes in the highly jointed and fractured welded tuff. Voids would cause thermal conductivity asymmetries and errors. In addition, we did not consider it desirable to fill the existing open fractures with grout because of chemical, thermal, mechanical, or permeability problems.

Therefore we potted the TCs into a 25.4-mm (1-in.) PVC pipe with the tips bent outward so they would rub against the rock and make good thermal contact. The TC tip and thermistor locations in these holes are listed in Table 8. We selected these locations to avoid large fractures and voids, which we determined through core logging and borehole television analysis.

Table 8. Thermocouple and Thermistor Location Depths in TH-1 and TH-2

Gage Depth (ft)	TH-1	TH-2
53.5	TC	-
56.5	TC	TC
58.5	Thermistor	TC
59.5	TC	Thermistor
60.0	-	TC
60.5	TC	TC
61.0	-	TC
61.5	TC	TC
62.0	-	TC
62.5	TC	TC
63.0	-	TC
63.5	TC	TC
64.5	TC	TC
65.5	-	TC
67.5	Thermistor	TC
69.5	TC	Thermistor

We placed rubber baffles along each TC string at several locations to minimize the effects of thermal convection along the holes. Steel leaf-spring centralizers maintained the strings' position in the hole and held the TCs against the hole wall. Shrink tubing on all the TCs in the strings—except in the region of the tips—provided electrical isolation of the TC sheaths. Sheath-to-sheath electrical resistance checks ensured that all TCs were making contact with the rock.

Originally we did not design an insertion tool. We were to insert the TC strings by pushing on the TC sheaths. However, we had difficulties in inserting the TCs to the desired depths and had to use black water pipe in addition to the PVC pipe to add stiffness and overcome the roughness of the holewall. During this process we inserted, extracted, and reinserted one of the strings. Thermocouples that had been bent during extraction had to be reconfigured to rub against the drill hole and reinserted at the proper depth.

Although the TCs were not individually calibrated, given material specifications, we could trace their measurements to NBS standards by using NBS polynomials which determine temperature from TC output voltages. All TCs seemed to operate normally throughout the entire experiment. Data from all over the array were consistent with their placement and with the expected thermal profiles. We recovered and visually inspected all the TCs and observed no corrosion. Some of the TC sheaths had been worn by abrasion during insertion and extraction. Several steel centralizer springs had broken, but we do not know the exact time of failure, although the cause seems to be related to stress-corrosion. The rubber baffles which had been used to minimize convection, may have helped keep the TC strings centralized; however consistency of TC data indicates that the failure occurred during recovery and not before.

Gas and Water Collection System

To sample gas and water from packed sections of any hole, we used stainless steel tubing and a valve and collection manifold in the instrumentation alcove. A vacuum pump and reservoir were used when a vacuum was needed. Pressure and vacuum gages diagnosed the gas and water collection system. Each hole had a 3.17-mm (0.125-in.) tube for gas sampling and both a 3.17-mm and a 6.35-mm (0.25-in.) tube for water sampling. The larger diameter tube was for standby use in case the smaller one should become plugged. It could also be used if water collected too fast for the small tube to drain, thus preventing damage to instrumentation in the hole.

We sampled gas by closing all valves to the array and then evacuating the sampling manifold and a 150-cm³, stainless-steel sampling cylinder. The vacuum system was then disconnected and the valve to the desired sample tube opened. After the sample was taken, we closed the valve and removed and labeled the sample cylinder. Gas samples were taken before the heater was powered, just before the heater was turned off, and before the instrumentation was removed.

Water sampling was somewhat similar to gas, the collection manifold and cylinder being evacuated when necessary. In some cases gravity flow was enough; a valve leading to the hole with the sample was opened and water ran into a calibrated buret. The water was transferred into plastic bottles, labeled, and saved for shipment to the laboratory.

Later, we devised a semi-automatic water sampling scheme; during nonworking hours, water was drawn from the heater hole upon command from the DAS and deposited in a large bottle (Figure A5). We then transferred it to plastic bottles, labeled them, and prepared them for shipment.

Power Distribution and Alarm System

In order for the experiment to succeed, power to the heater had to be uninterrupted and the DAS had to operate continuously. Also, the temperature of the rocks in the heater holes had to be prevented from exceeding design limits, water had to be extracted successfully, and the safety of personnel had to be emphasized.

Power requirements were met by the power distribution and alarm system. We expended considerable effort to provide an autostart, backup heater power system and uninterruptable power for the DAS. We installed alarms—automatic telephone messages, and computer-based—to warn of power outages, temperature excursions, and potential pressure safety problems.

A start-on-demand diesel generator (Figure 13) provided heater power in case commercial power was lost. (Heater power loss for more than a few seconds could have caused TC measurement fluctuations not only in the heater hole, but also in adjacent holes.) We positioned the diesel and its sensing, starting, and switch gear at the G-tunnel portal and ran special instrument power lines to a substation near the alcove, a run of about 1.9 km (1.25 mi).

If, for any reason, instrument power was lost to the heater alcove, the diesel would automatically furnish regulated instrument power to the alcove, nominally within 10 s.

Uninterruptable power was also required for the HP9845T data acquisition controller because even transient power outages would cause loss of the volatile memory and hence, data. Autostart capabilities could reset the memory and start collecting data again, but loss of some data was possible if even short-term power outages occurred.

The uninterruptable power supply used was an Elgar Model UP2500, rated at 2.5 kW. Tests conducted with the system load showed that there was no appreciable ac voltage drop after 7 h of running on rechargeable batteries, with no input power. The power supply uses a dc-to-ac converter that changes about 90 V dc to isolated 115-V ac, 60-Hz power. During normal operation the batteries are continuously charged by the input ac power. When input power is lost, the batteries immediately supply uninterrupted power to the converter. A reverse-transfer switch transfers power back to normal line power only if the uninterruptable power supply itself fails.

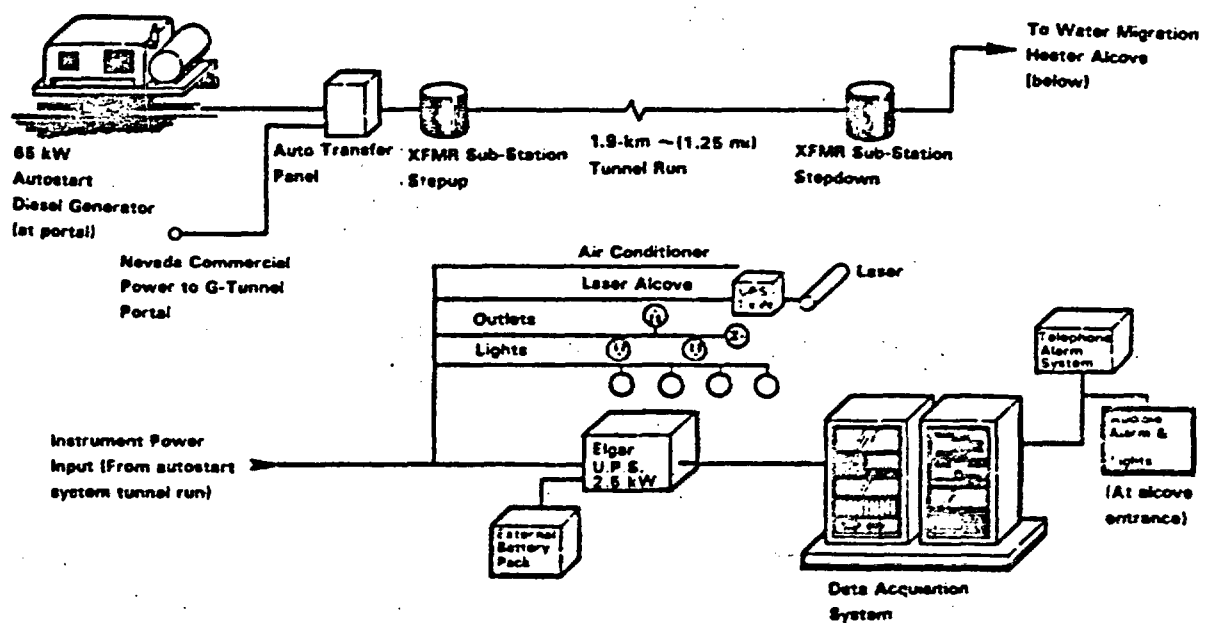

Figure 13. Power Distribution System and Alarms

To cover long periods (such as weekends) when the experiment was to run unattended, we installed an alarm system to alert us if power was lost. The telephone dialer alarm used was a Model L700D, supplied by Acro-Larm. It was connected to heater rock-wall temperature output in order to insure that temperatures did not exceed limits that could cause degradation of the heater hole rock wall. In addition, power outage messages and alarms were recorded.

The alarm system consisted of a preprogrammed, continuous-loop tape cartridge that had the telephone numbers of personnel and messages prerecorded on two tracks, each of which could be triggered independently of the other and which could contain different numbers and wording. The continuous-loop took about 5 min to run and could easily accept up to about five different phone numbers and messages per track. The system operated satisfactorily.

The HP3052A DAS could also determine if overtemperatures existed. Also, CRT messages, audible alarms, and relay closures for lighted alarms outside the alcove indicated potentially dangerous pressures measured in any of the holes.

Conclusions

In general the instrumentation designed and fielded for the In-Situ Tuff Water Migration/Heater Experiment operated as designed:

- The pH sensors operated nominally with qualifications based on the fielding conditions.
- Some of the pressure transducers failed, but late in the test.
- The laser strainmeter demonstrated its sensitivity, but its counting electronics and mounting design must be modified before it can yield quantitative results.
- The RH sensors did not operate satisfactorily
- Though the output of the water-level was not repeatable during the experiment because of pin coating, it was useful to indicate changes in water levels.
- The DAS performed well under less-than-ideal conditions; only minor hardware problems were encountered and problems with the software resulted from on-line development testing of improvements, and expanded capabilities.
- The water collection system, TCs, and stressmeters seemed to have operated without difficulties.

References

[1]J. K. Johnstone, *In-Situ Tuff Water Migration/Heater Experiment: Experimental Plan*, SAND79-1276 (Albuquerque: Sandia National Laboratories, August 1980).

[2]J. L. Krumhansl, *Final Report: Conasauga Near Surface Heater Experiment*, SAND79-1855 (Albuquerque: Sandia Laboratories, November 1979).

[3]A. R. Lappin, R. K. Thomas, and D. F. McVey, *Eleana Near-Surface Heater Experiment Final Report*, SAND80-2137 (Albuquerque: Sandia National Laboratories, April 1981).

[4]J. K. Johnstone, *In-Situ Tuff Water Migration/Heater Experiment: Final Report*, SAND81-1918 (Albuquerque: Sandia National Laboratories, Nd). To be published.

[5]C. O. Duimstra, *In-Situ Tuff Water Migration/Heater Experiment: Hardware Mechanical Design Definition*, SAND81-1048 (Albuquerque: Sandia National Laboratories, November 1981).

[6]J. Berger and R. H. Lovberg, "Earth Strain Measurements with a Laser Interferometer," *Science* 170:296, October 1970.

[7]C. W. Cook and E. S. Ames, *Borehole-Inclusion Stressmeter Measurements in Bedded Salt*, SAND79-0377 (Albuquerque: Sandia National Laboratories, July 1980).

[8]D. R. Waymire and C. O. Duimstra, *In-Situ Tuff Water Migration/Heater Experiment: The Data Acquisition and Playback System*, SAND81-1059 (Albuquerque: Sandia National Laboratories, October 1981).

[9]*Operations Manual For Digital Humidity & Temperature Measurement System Model HS-2CHDT-2A To Include: Discrete Relative Humidity Transducers Model RHT-500 S/N 501, 502* (Albuquerque: Thunder Scientific Corp, September 24, 1979).

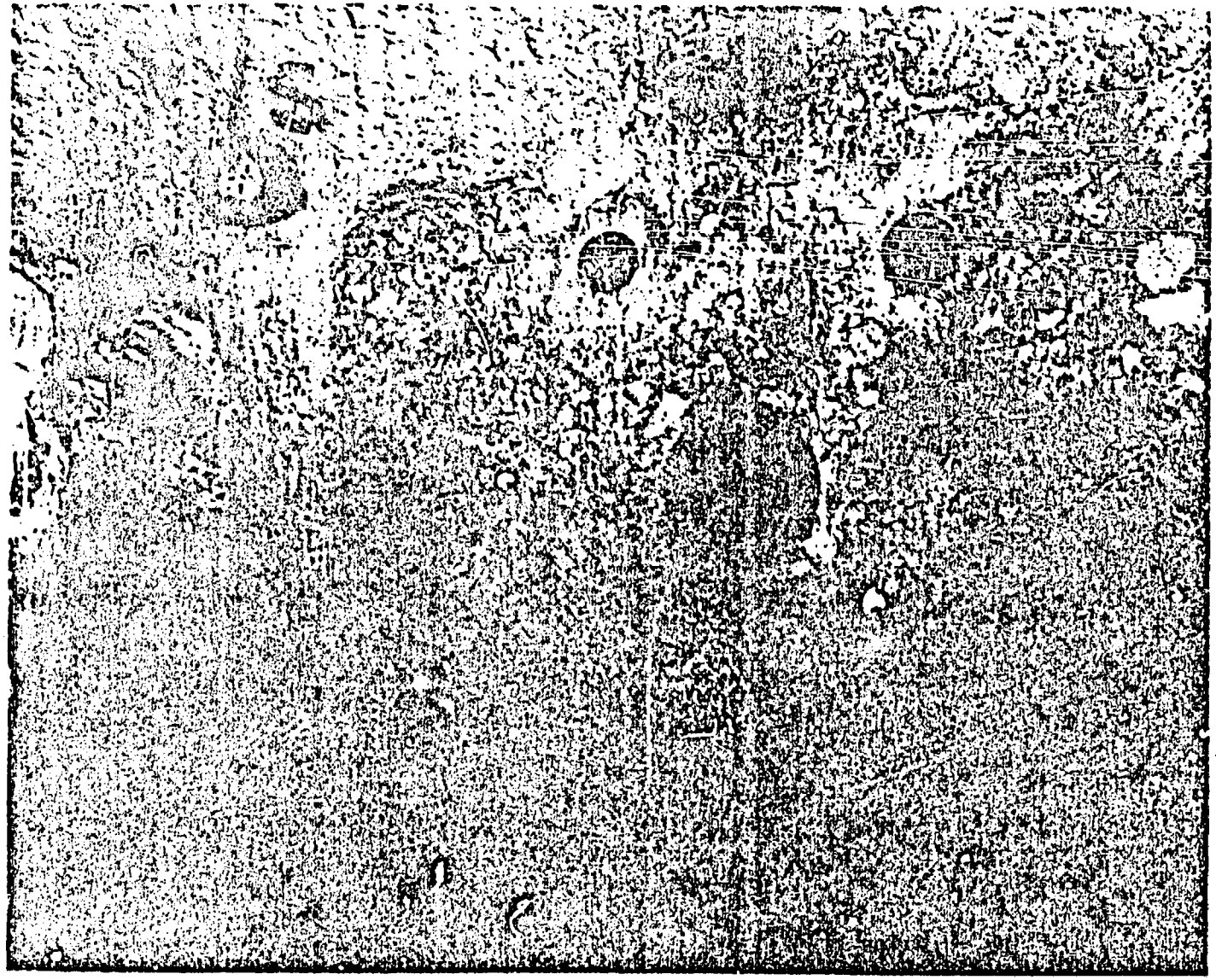

Figure A1. Drill Hole Pattern for the Heater Array (Black hole contains cables for installed stressmeters.)

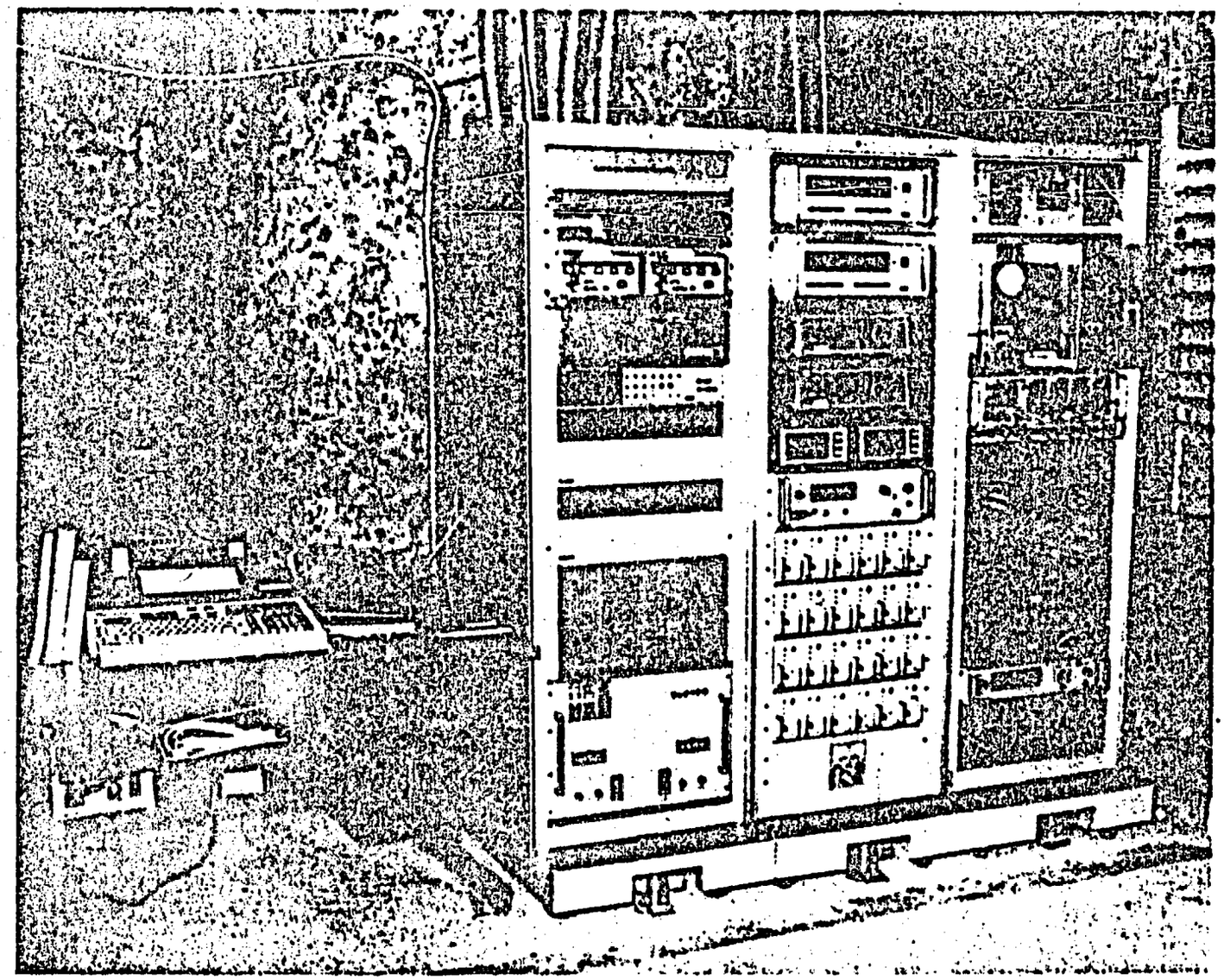

Figure A2. Data Acquisition System (featuring an HP9845 and HP3052A system. Also seen are Elgard uninterruptable power supply, telephone alarm system, signal conditioning and data readout hardware.)

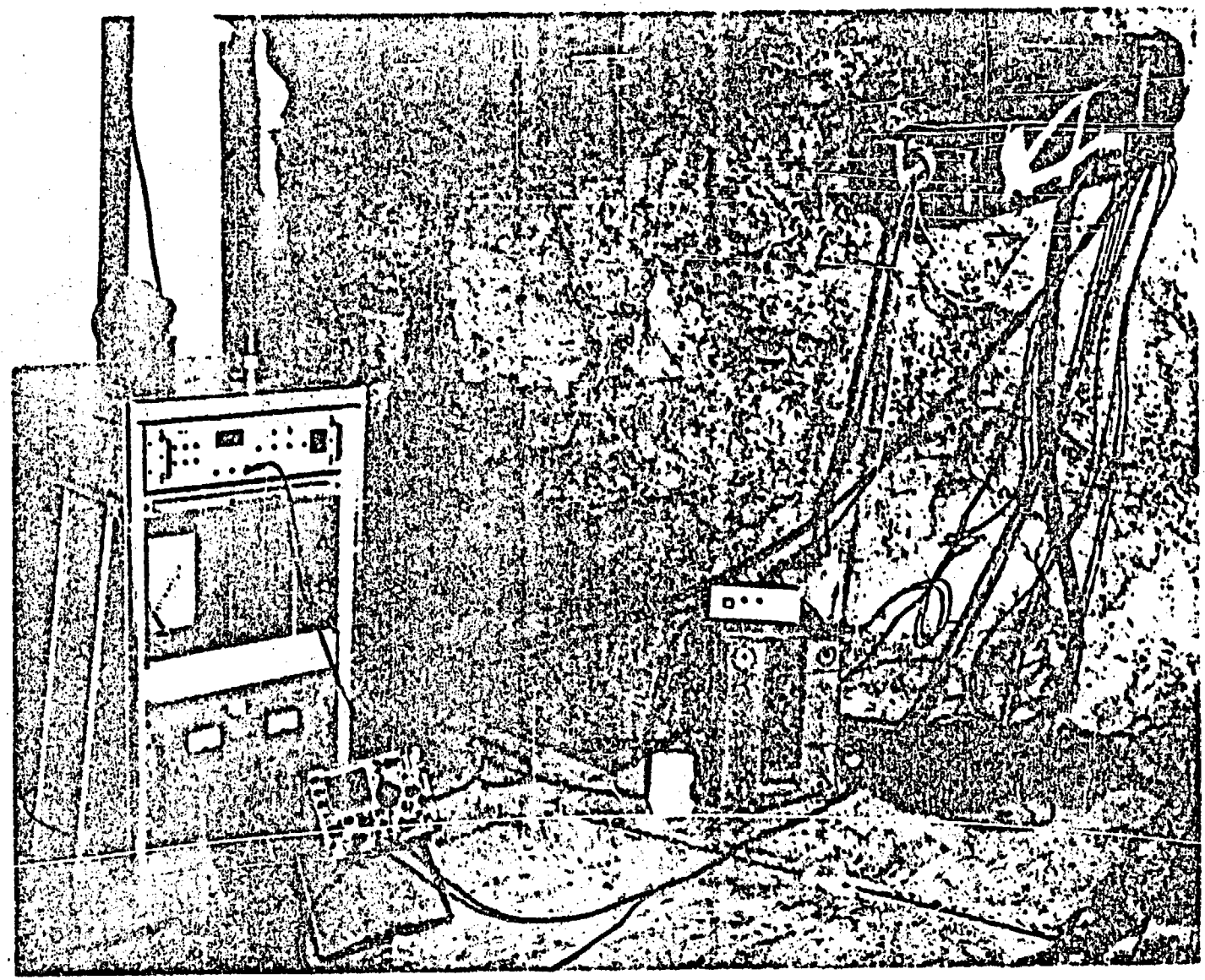

Figure A3. The Laser Alcove Where the Laser Head is Mounted on the Rock Wall (Included in the photo are the electronic counting system, power supplies, and test equipment.)

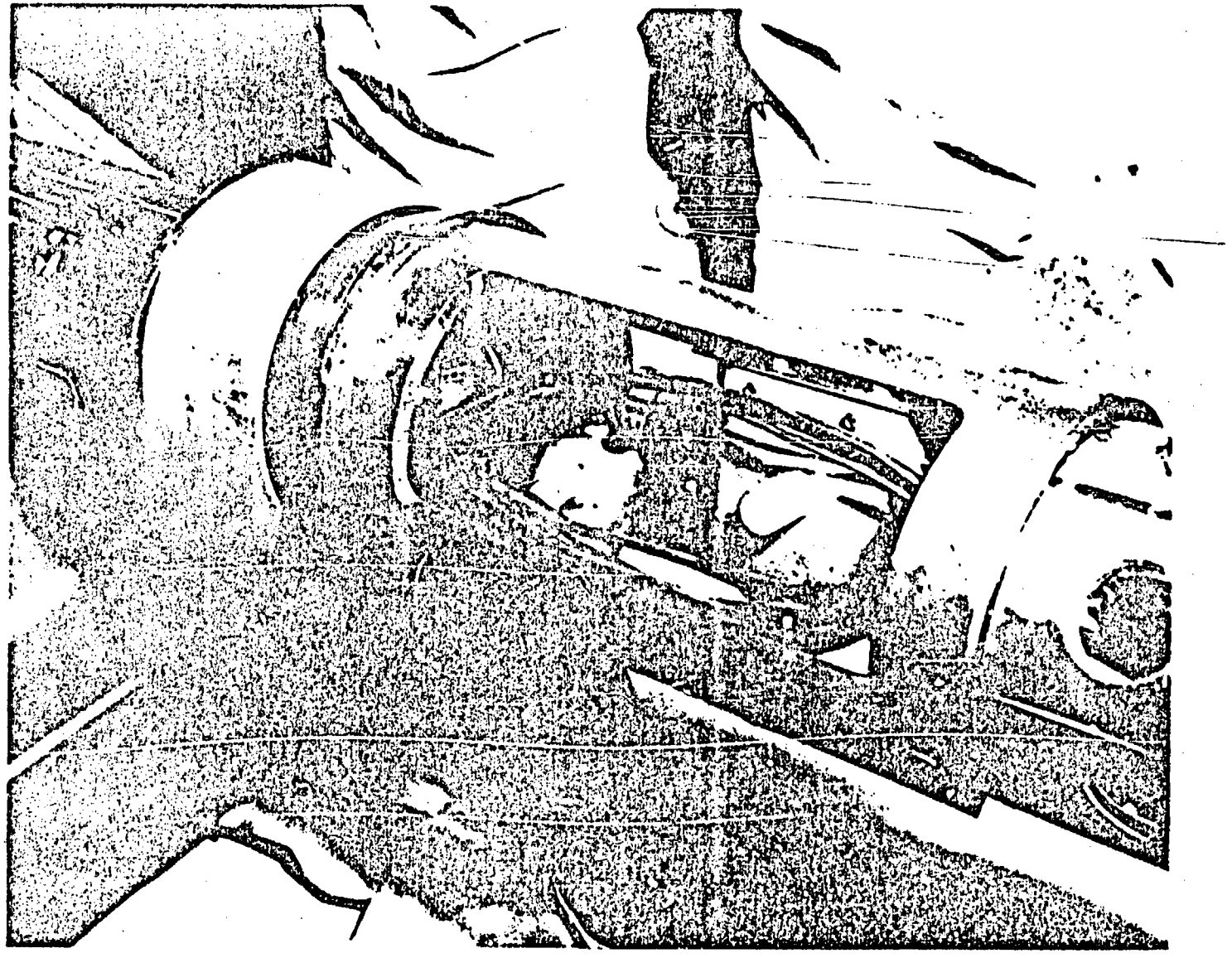

Figure A4. The Instrumentation Section of the Heater Assembly, Showing the Scum on the Water Level Indicator (This photo taken immediately after recovery.)

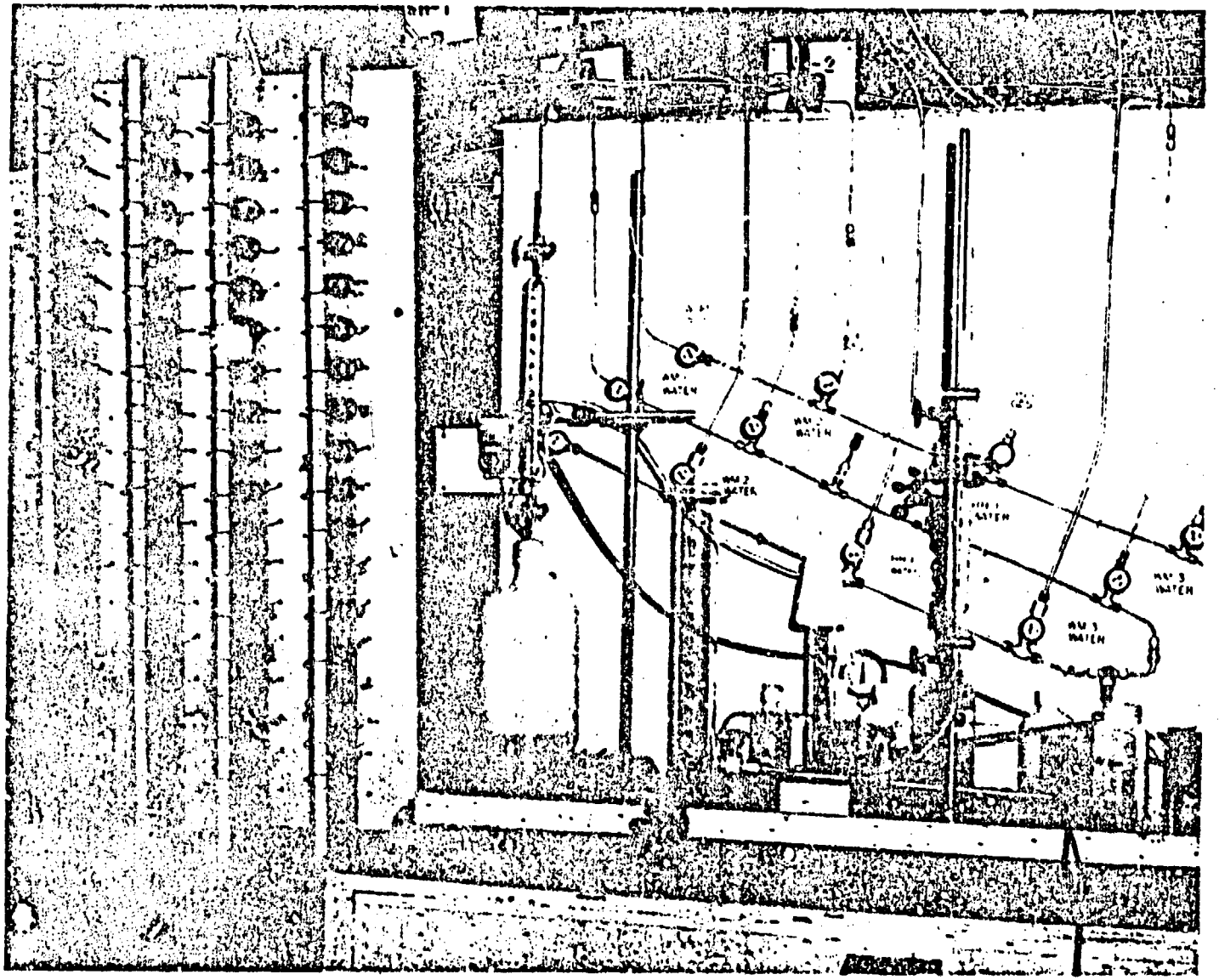

Figure A5. The Gas and Water Sampling Manifold, Including the Automated System